Guided Waves on a Planar Helix

SHEEL ADITYA, STUDENT MEMBER, IEEE, AND RAJENDRA K. ARORA, SENIOR MEMBER, IEEE

Abstract—**Considered here is a planar structure comprising a pair of parallel arrays of periodically spaced conducting strips which conduct in different directions in the two arrays. The guiding properties of this planar structure are found to be similar, in one case, to those of circular tape helices. While in general, different dielectric media are assumed in the sandwiched and outer regions, the special cases studied are 1) the case in which air constitutes both the media, 2) the normal-helix case in which the inner medium is a solid dielectric and the outer medium is air, and 3) the "inverted-helix" case with the two media interchanged.**

I. Introduction

THE conducting helix of circular cross section has certain unique properties, such as large bandwidth and low dispersion, which have led to its widespread use (see, for example, [1]). A somewhat related slow-wave structure in planar geometry was considered in [2] and [3]. It consisted of a pair of parallel unidirectionally conducting screens, each conducting in a different direction. In [3], the structure was confined in the transverse direction by metal planes; this made exact analysis difficult and recourse had to be taken to a variational approach. While the excitation characteristics of the infinitely wide structure were studied in [4], the dispersion curves for a generalization of this structure were reported in [5]. In the following this structure is referred to as a "planar helix".

As in the case of initial studies on the circular helix, so far the planar helix has been studied in the sheath-helix approximation. Although this approximation revealed the potential of the planar helix as a planar slow-wave structure, the details of the dispersion curves were obscured because of the limitations resulting from the omission of the periodic character of the structure as well as the finite conductor width. Since these aspects can have an important bearing on the behavior of the structure, it is desirable that the effect of these be incorporated in the analysis. To this end, an approach similar to the "tape-helix" model [6], [7] is used here; space harmonics, the forbidden region, as well as other details, appear quite naturally as a consequence of this model. It may be noted that a related coaxial structure consisting of crosswound helical wires surrounding a central conductor has been studied by Wait [8].

Manuscript received January 15, 1979; revised June 11, 1979.

S. Aditya is with the Centre for Applied Research in Electronics, Indian Institute of Technology, New Delhi 110029.

R. K. Arora is with the Department of Electrical Engineering, Indian Institute of Technology, New Delhi 110029.

II. Configuration

The structure considered here for analysis consists of a pair of arrays of parallel, straight, and perfectly conducting strips. The strips are assumed to be infinitesimal in thickness. Along the x direction, the arrays are separated by a distance $2a$ (Fig. 1). For simplicity, the structure is taken to be infinitely wide in the y direction. However, it seems reasonable to expect that the results obtained here will be applicable to a structure many wavelengths wide. Strips in the top array are oriented at an angle α, while those in the bottom array are oriented at an angle $-\alpha$, with respect to the y axis. The directions parallel to the strips in the top and bottom arrays are called y' and y'', respectively. With the choice of the axes as shown, the center lines of the strips intersect the axes at $y = mp_y$ and $z = np_z$, where m and n are integers, and p_y and p_z are the periodic spacings between the strips measured along y and z directions, respectively; p_y and p_z are related as $p_z/p_y = \tan\alpha$. Similarly, the stripwidth w is related to w_y and w_z as $w_y = w/\sin\alpha$ and $w_z = w/\cos\alpha$. In general, the permittivities of medium 1 and 2 are considered to be different.

III. Symmetry Properties

The planar helix remains unchanged under any one or any combination of the following transformations:

$$(x,y,z) \longrightarrow (-x,-y,z) \tag{1a}$$

$$(x,y,z) \longrightarrow (x, y \pm p_y/2, z + p_z/2). \tag{1b}$$

The transformation (1a) rotates the structure about the z axis by 180°. When this is considered together with Maxwell's equations, one finds that the solution of the problem must be either even or odd if x and y are taken in conjunction [9]. Thus the structure admits of two independent solutions: transverse symmetric and transverse antisymmetric. For the two solutions, the fields have :

$$\begin{aligned} \begin{matrix} E_x \\ H_x \end{matrix}(x,y,z) &= \pm \begin{matrix} E_x \\ H_x \end{matrix}(-x,-y,z) \\ \begin{matrix} E_y \\ H_y \end{matrix}(x,y,z) &= \pm \begin{matrix} E_y \\ H_y \end{matrix}(-x,-y,z) \\ \begin{matrix} E_z \\ H_z \end{matrix}(x,y,z) &= \mp \begin{matrix} E_z \\ H_z \end{matrix}(-x,-y,z). \end{aligned} \tag{2}$$

In (2) upper signs apply to the transverse-symmetric solution.

0018-9480/79/1000-0860$00.75 ©1979 IEEE

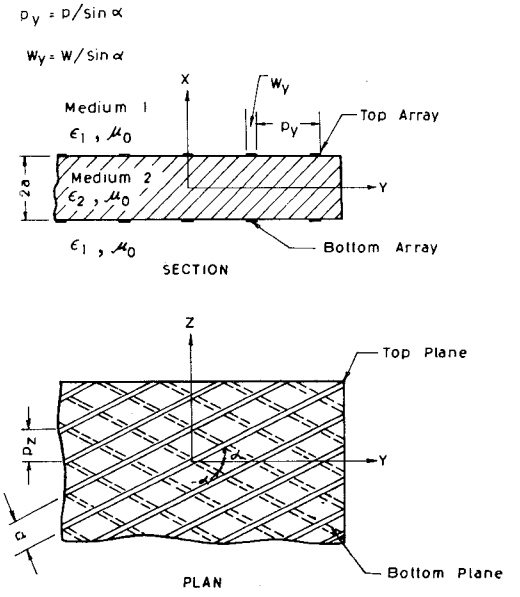

Fig. 1. Cross section of the planar helix; z is the direction of propagation.

The invariant transformation (1b) is shared in common with crosswound twin helices described by Chodorow and Chu [7]. Therefore, the forms of the exponent used in the field expressions there should be applicable here also. Moreover, the symmetry implied by (1a) ensures that only one half of the structure need be considered for a solution. Finally, the field expressions constituting the solution should reflect the periodicity of the structure—in both y and z directions.

IV. Field Expressions, Boundary Conditions

In the following, the time-dependence factor $\exp(j\omega t)$ is assumed to multiply all the field quantities. The direction of propagation is taken to be $+z$. From (1) and (2), field expressions appropriate for region 2 for the transverse-symmetric case are

$$E_{z\mathrm{II}} = \sum_{m=-\infty}^{\infty}\sum_{n=-\infty}^{\infty}\left[C_{mn}\sinh(k_{mn}x)\cos\left(\frac{2\pi ny}{p_y}\right) + C'_{mn}\cosh(k_{mn}x)\sin\left(\frac{2\pi ny}{p_y}\right)\right]e^{-j\beta_{mn}z} \quad (3a)$$

$$H_{z\mathrm{II}} = \sum_{m=-\infty}^{\infty}\sum_{n=-\infty}^{\infty}\left[D_{mn}\sinh(k_{mn}x)\cos\left(\frac{2\pi ny}{p_y}\right) + D'_{mn}\cosh(k_{mn}x)\sin\left(\frac{2\pi ny}{p_y}\right)\right]e^{-j\beta_{mn}z}. \quad (3b)$$

Similarly for region 1, considering that the fields decay away from the structure:

$$E_{z\mathrm{I}} = \sum_{m=-\infty}^{\infty}\sum_{n=-\infty}^{\infty}\left[A_{mn}\cos\left(\frac{2\pi ny}{p_y}\right) + A'_{mn}\sin\left(\frac{2\pi ny}{p_y}\right)\right]e^{-\alpha_{mn}(x-a)}e^{-j\beta_{mn}z} \quad (3c)$$

$$H_{z\mathrm{I}} = \sum_{m=-\infty}^{\infty}\sum_{n=-\infty}^{\infty}\left[B_{mn}\cos\left(\frac{2\pi ny}{p_y}\right) + B'_{mn}\sin\left(\frac{2\pi ny}{p_y}\right)\right]e^{-\alpha_{mn}(x-a)}e^{-j\beta_{mn}z}. \quad (3d)$$

In (3), α_{mn}, restricted to be positive and real, are given by

$$\alpha_{mn}^2 = (2\pi n/p_y)^2 + (\beta_{mn})^2 - k_{\mathrm{I}}^2 \quad (4a)$$

$$k_{mn}^2 = (2\pi n/p_y)^2 + (\beta_{mn})^2 - k_{\mathrm{II}}^2 \quad (4b)$$

$$\beta_{mn} = \beta_{00} + (2\pi/p_z)(2m+n) \quad (4c)$$

$$k_{\mathrm{I}}^2 = \omega^2\mu_0\epsilon_0\epsilon_{r1}, \qquad k_{\mathrm{II}}^2 = \omega^2\mu_0\epsilon_0\epsilon_{r2}. \quad (4d)$$

In the transverse-antisymmetric case, cosh replaces sinh and vice versa.

The x and y components of the electric and magnetic fields in the two regions are obtained by using Maxwell's equations. The coefficients $A_{mn}, A'_{mn}, \cdots$, etc., involved in the expressions for these components are related by the following boundary conditions: the tangential components of the electric field are continuous at $x=a$, and

$$H_{y\mathrm{I}} - H_{y\mathrm{II}} = J_z \quad (5a)$$

$$H_{z\mathrm{II}} - H_{z\mathrm{I}} = J_y \quad (5b)$$

where J_z and J_y are the components of the surface current density on the surface $x=a$. Further, assuming that the strips are narrow compared to the period, the separation of the arrays and the wavelength, from physical considerations, it can be assumed that the current flows essentially longitudinally along the strips, i.e.,

$$J = J_{y'} \quad (6a)$$

so that

$$J_z = J_{y'}\sin\alpha \quad \text{and} \quad J_y = J_{y'}\cos\alpha. \quad (6b)$$

Analogous to (3), $J_{y'}$ is expressed in the form

$$J_{y'} = \sum_{m=-\infty}^{\infty}\sum_{n=-\infty}^{\infty}\left[J_{mn}\cos\left(\frac{2\pi ny}{p_y}\right) + J'_{mn}\sin\left(\frac{2\pi ny}{p_y}\right)\right]e^{-j\beta_{mn}z}. \quad (7)$$

By applying the boundary conditions mentioned earlier, one evaluates the coefficients $A_{mn}, A'_{mn}, \cdots$, etc., in terms of J_{mn} and J'_{mn}.

V. Characteristic Equation

To arrive at the dispersion relation for the structure, the variational technique introduced in [7] is found suitable here also. Let I represent the complex power which might be generated or absorbed by the top array. Then

$$I = \int_{-p_z/2}^{p_z/2}\int_{-p_y/2}^{p_y/2}\left[E_z(H_{y\mathrm{I}}^* - H_{y\mathrm{II}}^*) + E_y(H_{z\mathrm{II}}^* - H_{z\mathrm{I}}^*)\right]dy\,dz. \quad (8a)$$

The field components above are evaluated at $x=a$. From

(5) and (6)

$$I=\int_{-p_z/2}^{p_z/2}\int_{-p_y/2}^{p_y/2}\left[E_z\sin\alpha+E_y\cos\alpha)J_{y'}^*\right]dy\,dz \quad (8b)$$

in which $J_{y'}$ is obtained from (7). Now, to obtain the dispersion relation one sets

$$\delta I(J_{mn}^*:J_{mn}'^*)=0. \quad (9)$$

For an approximate solution, one may assume $J_{y'}$ to consist of a finite number of terms. For similar problems meaningful results have been obtained by single-term approximations [6], [7]. Accordingly, the results reported here are based on the following single-term approximation:

$$J_{y'}=J\exp(-j\beta_{00}yp_z/p_y)yp_z/p_y-w_z/2<z<yp_z/p_y+w_z/2$$
$$=0 \quad \text{elsewhere.} \quad (10)$$

In this "zeroth-order" approximation the characteristic equation reduces to a singly infinite series with $m=0$. For instance, for the case when $\epsilon_{r1}=\epsilon_{r2}=1$, the characteristic equation is

$$\sum_{n=-\infty}^{\infty}\left[-\frac{\omega\mu_0 k_{0n}\cos\alpha}{k_c^2}(B_{0n}'+jB_{0n})+\left(\frac{\beta_{0n}2\pi n/p_y\cos\alpha}{k_c^2}+\sin\alpha\right)(A_{0n}-jA_{0n}')\right]=0. \quad (11)$$

VI. Forbidden Region

Before passing on to results obtained by numerical solutions of the characteristic equation, it should be of interest to consider the forbidden region for the planar helix. Since only those solutions are sought for which the fields decay away from the arrays, it is implied that none of the α_{mn} can be imaginary or negative for an acceptable solution. This restriction results in a forbidden region the boundary of which, for the present single-term approximation, is determined as follows:

$$(\beta_{0n})^2+(2\pi n/p_y)^2-k_I^2\geq 0\ . \quad (12a)$$

which, together with (4c), yields

$$\beta_{00}p_z/2\pi\geq -n\pm\left[(k_0p_z/2\pi)^2\epsilon_{r1}-(n\tan\alpha)^2\right]^{1/2}. \quad (12b)$$

Figs. 2 and 3 include the plots of forbidden regions for $\epsilon_{r1}=1$ and 2.56, respectively, and α is taken as 10°. Evidently, the forbidden region changes with α. The troughs in the boundary are given by

$$\left[k_0p_z/2\pi,\beta_{00}p_z/2\pi\right]=\left[n\tan\alpha/(\epsilon_{r1})^{1/2},n\right]. \quad (12c)$$

Solutions for slow-wave propagation must fall below the boundary of the forbidden region.

VII. Numerical Results

For the numerical solution of the characteristic equation, values assumed for various parameters are $\alpha=10°$, $w_z/p_z=0.1$ and $p_z/2\pi a=1$. The infinite series in the characteristic equations is found to converge sufficiently fast to truncate the series after five terms.

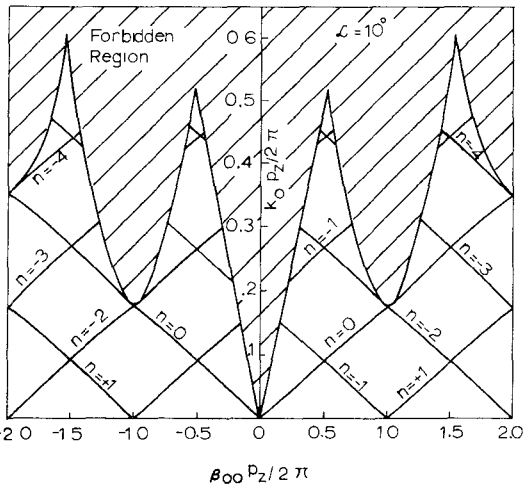

Fig. 2. Forbidden region for $\epsilon_{r1}=1$ and $\alpha=10°$. Also shown are the dispersion characteristics for the air case: $\epsilon_{r1}=\epsilon_{r2}=1$. Different space harmonics are marked by different values of n.

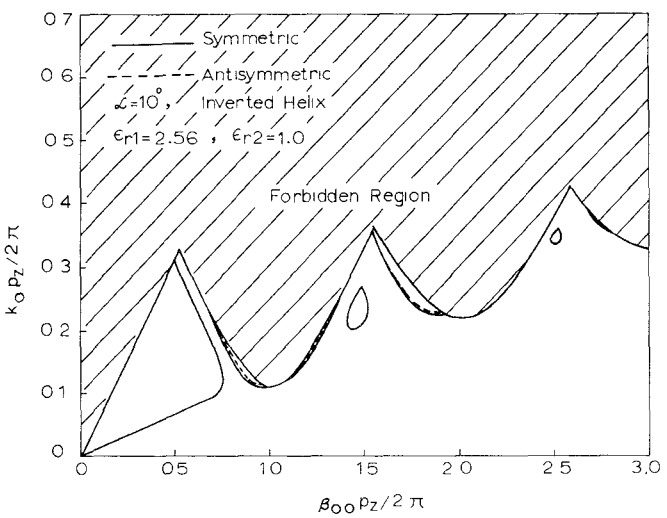

Fig. 3. Forbidden region for $\epsilon_{r1}=2.56$ and $\alpha=10°$. Also, dispersion characteristics for the inverted-helix case: $\epsilon_{r1}=2.56$, $\epsilon_{r2}=1$, $\alpha=10°$. Dashed curves represent the transverse-antisymmetric solution where it is different from the symmetric one.

Fig. 2 presents the results for the case when there is air in between and outside the arrays. Various space harmonics are indicated by different values of n. The fundamental space harmonic runs continuous, unlike in the case of circular tape helices where a break occurs because of the forbidden region. The curve for this case is tangential to the troughs in the forbidden region, and closely follows the straight line $k_0p_z/2\pi=\sin\alpha(\beta_{00}p_z/2\pi)$. Also, the symmetric solution is identical to the antisymmetric one. This appears to be a consequence of the approximation for $J_{y'}$ used here. In any case, as seen in the sheath-helix approximation [2], the difference between the two solutions is small and it decreases as frequency increases. For a more accurate solution, a general approximation for $J_{y'}$

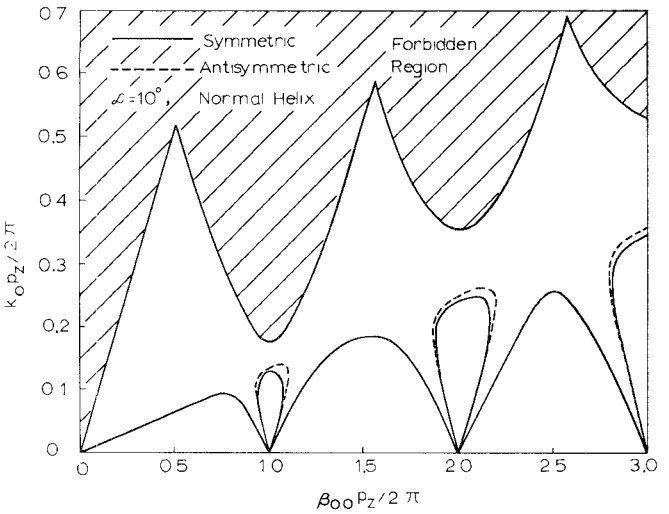

Fig. 4. Fundamental space harmonic for the normal-helix case: $\epsilon_{r1}=1$, $\epsilon_{r2}=2.56$, $\alpha=10°$. Dashed curves represent the transverse-antisymmetric solution where it is visibly different from the transverse-symmetric one.

is as follows:

$$J_{y'}=\sum_{m=m'}^{m''}\sum_{n=n'}^{n''}\left[G_{mn}\sin(2\pi ny/p_y)+H_{mn}\cos(2\pi ny/p_y)\right]e^{-j\beta_{mn}z}\quad\text{on the strips}$$
$$=0\quad\text{elsewhere.}\qquad(13)$$

Fig. 4 gives the dispersion curves for the case when region 2 is filled with polystyrene ($\epsilon_{r2}=2.56$). This is the "normal-helix" case. For the sake of clarity only β_{00} is plotted. Wherever the antisymmetric solution is visibly different from the symmetric one, it is shown by dashed lines; elsewhere the numerical difference is negligible. Only the lobes centered around $\beta_{00}p_z/2\pi=n$ ($n=1,2,3,\cdots$) are different in the two cases. Even this difference gradually decreases as n increases. The top portions of various parts of the fundamental tend to follow a common "envelope". This fictitious envelope is lower than the fundamental in the air case. This is expected due to the presence of the dielectric. While in the air case there do not appear any branches deviating from the envelope, here it is seen that as the dielectric constant of region 2 is gradually increased, the various branches of the fundamental deviate more and more from the envelope.

Complementary to the normal-helix case, in the "inverted-helix" case region 1 consists of dielectric which again is taken to be polystyrene. Dispersion curves for both the symmetric and the antisymmetric cases are given in Fig. 3. As before, the dashed curves represent the antisymmetric solution where it is different from the symmetric solution. In this case also the difference between the two solutions decreases as $\beta_{00}p_z/2\pi$ increases. It should be noticed that the valleys in the forbidden-region boundary are lower in this case compared to the normal helix. Also, the deviation from the abovementioned fictitious common envelope is in the direction opposite to that in the normal helix. These two effects combine to cause the fundamental dispersion curve to merge with the forbidden-region boundary for large $\beta_{00}p_z/2\pi$.

Both the normal- as well as the inverted-helix cases admit the possibility of backward wave propagation. The appearance of closed lobes in the ω–β diagrams implies that ω becomes a double-valued function of β. Peculiarities like this are known to occur in doubly periodic structures [10].

VIII. Conclusion

An attempt has been made to study the dispersion characteristics of a planar helix, taking into account the effects of periodicity and a finite conductor width. These characteristics are found to exhibit the familiar space harmonics and forbidden region in the k–β diagram. The dispersion characteristics for the air case resemble the corresponding characteristics for a circular tape helix. This suggests that the planar helix in this form can have applications similar to those of its circular counterpart.

A similar comparison has not been possible in the dielectric case. Nonetheless, as mentioned in [5], possible application of this planar slow-wave structure, which is expected to involve an easier fabrication, can be in nonreciprocal ferrite components. This possibility is pursued further in some detail in [11] where a sheath helix on a pair of magnetized ferrite slabs is considered.

References

[1] D. A. Watkins, *Topics in Electromagnetic Theory*. New York: Wiley, 1958.
[2] R. K. Arora, "Surface waves on a pair of parallel unidirectionally conducting screens," *IEEE Trans. Antennas Propagat.*, vol. AP-14, pp. 795–797, Nov. 1966.
[3] E. A. Ash, "A new type of slow-wave structure for millimetre wavelengths," *Proc. Inst. Elect. Eng.*, vol. 105, Part B, no. 11, pp. 737–745, May 1958.
[4] R. K. Arora, "Field of a line source situated parallel to a surface-wave structure comprising a pair of unidirectionally conducting screens," *Can. J. Phys.*, vol. 45, 2145–2172, June 1967.
[5] R. K. Arora, B. Bhat, and S. Aditya, "Guided waves on a flattened sheath-helix," *IEEE Trans. Microwave Theory Tech.*, vol. MTT-25, pp. 71–72, Jan. 1977.
[6] S. Sensiper, "Electromagnetic wave propagation on helical structures," *Proc. IRE*, pp. 149–161, Feb. 1955.
[7] M. Chodorow and E. L. Chu, "Crosswound twin helices for travelling-wave tubes," *J. Appl. Phys.*, vol. 26, pp. 33–43, Jan. 1955.
[8] J. R. Wait, "Electromagnetic theory of the loosely braided coaxial cable: Part I," *IEEE Trans. Microwave Theory Tech.*, vol. MTT-24, pp. 547–553, Sept. 1976.
[9] C. G. Montgomery, R. H. Dicke, and E. M. Purcell, *Principles of Microwave Circuits*. M.I.T. Radiation Lab. Series, 8, McGraw-Hill, 1951.
[10] L. Brillouin, *Wave Propagation in Periodic Structures*. New York: McGraw-Hill, 1946.
[11] S. Aditya and R. K. Arora, "Nonreciprocal dispersion characteristics of a planar helix on magnetized ferrite slabs," pp. 864–868, this issue.